2010

Design of High-Sensitivity Plasmonics-Assisted GaAs Metal-Semiconductor-Metal Photodetectors.

Ayman Karar
Edith Cowan University, ayman_karar@hotmail.com

Narottam Das
Edith Cowan University

Chee Leong Tan

Kamal Alameh
Edith Cowan University, k.alameh@ecu.edu.au

Yong Lee
Edith Cowan University

10.1109/HONET.2010.5715761

Design of High-Sensitivity Plasmonics-Assisted GaAs Metal-Semiconductor-Metal Photodetectors

Ayman Karar[1*], Narottam Das[1], Chee Leong Tan[2], Kamal Alameh[1,4]* and Yong Tak Lee[2,3,4]

[1]Electron Science Research Institute, Edith Cowan University, 270 Joondalup Dr, Joondalup, WA 6027, Australia
[2]School of Photonics Science, Gwangju Institute of Science and Technology (GIST), 261 Cheomdan-gwagiro (Oryong-dong), Buk-gu, Gwangju, 500-712, Republic of Korea
[3]Department of Information and Communications, GIST; [4]Department of Nanobio Materials and Electronics, GIST
Phone: +61 8 6304 5836, Fax: +61 8 6304 5302, *email: k.alameh@ecu.edu.au, akarar@our.ecu.edu.au

***Abstract*—In this paper, we use the finite difference time-domain (FDTD) method to optimize the light absorption of an ultrafast plasmonic GaAs metal-semiconductor-metal photodetector (MSM-PD) employing metal nano-gratings. The MSM-PD is optimized geometrically, leading to improved light absorption near the designed wavelength of GaAs through plasmon-assisted electric and magnetic field concentration through a subwavelength aperture. Simulation results show up to 10-times light absorption enhancement at 867 nm due to surface plasmon polaritons (SPPs) propagation through the metal nano-grating, in comparison to conventional MSM-PD.**

***Index Terms*— Subwavelength aperture, surface plasmon polaritons, plasmonic nanostructures, nanophotonics, FDTD simulation, MSM-PD.**

I. INTRODUCTION

Metal-semiconductor-metal photodetectors (MSM-PDs) are very attractive devices for optical fiber communication systems, high-speed chip-to-chip connections, and high-speed sampling [1-2]. The operation of an MSM-PD can be classified into two groups, according to whether its intrinsic speed is limited by recombination time or transit time. In the first group, a large number of recombination centers have to be introduced into the active area to shorten the carrier recombination time for high-speed operation at the expense of low sensitivity and less compatibility with field effect transistor integrated circuit fabrication. In the second group, small finger spacing is utilized to decrease the transit time and increase the device speed [3]. For MSM-PDs, the smaller the spacing, the shorter intrinsic response time is. Furthermore, for the recombination time-limited photodetectors, smaller finger spacing can increase the sensitivity. On the other hand, the smaller finger width, the less detector capacitance and the shorter external response time. However, the downsizing of the electrode spacing leads to a decreased active area resulting in sensitivity degradation.

Since the Extraordinary Optical Transmission (EOT) phenomenon was first reported by Ebbesen et al. [4], many efforts have been devoted to exploring the EOT through metallic gratings with various sub-wavelength structures, such as periodic slit arrays, hole arrays, and corrugated metal films for different wavelength regions [5]. Recently, investigating the role of surface plasmon (SP) in periodic structures has become a major research topic. It has also been established that the transmission of light through a hole (or slit) in a metal film can be enhanced by microstructuring the top or bottom surfaces of the film with gratings. These gratings couple the incident light to surface plasmon polaritons (SPPs) that are guided into the holes [6-8].

The application of SPPs for enhancing the light transmission or absorption using subwavelength apertures has promised a large enhancement in light transmission. A new technique has been reported by Collin et al. [9] for efficient light absorption in MSM-PDs. They confirmed that the confinement of light in subwavelength metal–semiconductor gratings can be achieved by Fabry–Pérot resonances involving vertical transverse magnetic and electric guided waves, thereby increasing the quantum efficiency. Recently, Tan et al. reported a semi-analytical model and a numerical modelling of light absorption in 980nm MSM-PDs with plasmonic nano-gratings using the finite difference time domain (FDTD) method [10].

In this paper, we use FDTD method to optimize the parameters of an ultrafast MSP-PD structure; such as subwavelength aperture depth, height of the nano-grating, duty cycle, and other structure parameters to improve the light absorption in the active area of the device. Our simulation results show that an ultrafast

978-1-4244-9924-3/10/$26.00 ©2010 IEEE

plasmonic MSM-PD structure can attain 10-times better absorption than conventional MSM-PDs, and this is mainly due to the extraordinary optical signal propagation through the metal nano-grating.

II. Design of Ultrafast MSM-PDs

For the design of an ultrafast MSM-PD structure, we used the FDTD method to explore the application of SPs to improve the light transmission through a subwavelength aperture. A conventional MSM-PD structure is shown in Fig. 1(a). It consists of a two metallic (Au) contacts separated by a subwavelength aperture of width $\mathbf{X_w}$ and height (thickness) $\mathbf{h_s}$. Fig. 1(b) shows an MSM-PD structure consisting of a subwavelength aperture sandwiched between linear metal nano-gratings of heights $\mathbf{h_g}$, and a period ($\mathbf{\Lambda}$) and a duty cycle of **X**%. The entire structure is grown on top of a semiconductor (GaAs) substrate

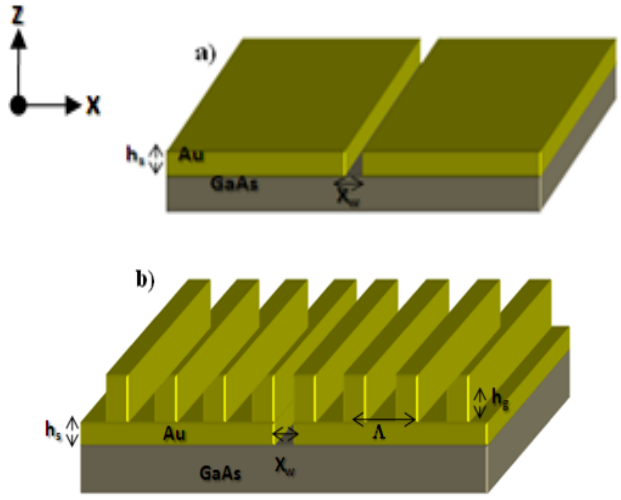

Fig. 1. (a) Simple MSM-PD structure without a plasmonic nano-grating, (b) MSM-PD structure with a linear plasmonic nano-grating.

The nano-corrugations are required in order to provide the momentum difference, satisfy the dispersion relation and allow collective resonant coupling between the incident light and electrons oscillation in the MSM-PD metal fingers. The metal nano-grating period $\mathbf{\Lambda}$ can be obtained from the following relation [10-11]

$$k_{\parallel} = k \sin\theta \pm \frac{2m\pi}{\Lambda} = \frac{\omega}{c}\sqrt{\frac{\varepsilon_m \varepsilon_d}{\varepsilon_m + \varepsilon_d}} = k_{sp} \qquad (1)$$

where k_{sp}, ω, θ and c are the SPPs wave vector, angular frequency, light incidence angle the speed of light in vacuum, respectively. The complex dielectric permittivity of the metal is defined as $\varepsilon_m = \varepsilon_m' + i\varepsilon_m''$ and that of the air is ε_d. Using equation (1), a period of $\mathbf{\Lambda}$ = 815 nm for the Au/air interface corresponds to a GaAs MSM-PD with an edge of absorption of around 830 nm for $\theta = 0$.

To maximize the light concentration effects, we combine two distinct mechanisms that relate to the presence of the subwavelength aperture and the nano-grating [12]. The metallic subwavelength aperture supports a propagating TE mode with the EOT. Consequently, with an appropriate choice of its width, the subwavelength aperture forms a Fabry–Pérot resonator; therefore, the light transmission through the subwavelength aperture is resonantly enhanced. On the other hand, the nano-grating enhances the light transmission through the subwavelength aperture region by converting the incident EM waves into SPs propagating on the metal surface, which can be funneled into the subwavelength aperture [13]. With an accurate choice of geometric parameters of the structure, these two mechanisms can occur at the same time, resulting in an enhanced efficiency of the device.

To design the MSM-PDs (with and without a metal nano-grating), we used a 2D FDTD models software that was developed by Optiwave Inc. The structure had a mesh step size of 10 nm and a time step satisfy the condition of $\delta t < 0.1\delta x/c$. This high-resolution sampling yielded solutions that converged at reasonable computation times. The excitation field was modeled as a Gaussian-modulated continuous wave in z-direction. The anisotropic perfectly matched layer (APML) boundary conditions were applied in both the x- and z- directions to accurately simulate the light reflected from the bottom and both sides, as well as light transmitted from the top boundaries of the MSM-PD structure. The gold (Au) dielectric permittivity was defined by the Lorentz-Drude model [14] and the GaAs dielectric permittivity data was taken from [15].

III. Results and Discussion

Initially, we used the conventional MSM-PD without grating (Fig. 1(a)) to optimize the subwavelength aperture height $\mathbf{h_s}$, because the transmission of light through the subwavelength aperture is strongly dependent on it. The height ($\mathbf{h_s}$) was varied between 50-120 nm with steps of 20 nm, while keeping the subwavelength aperture width $\mathbf{x_w}$ constant at 100 nm. The calculated normalized transmitted power (normalized to the incident power) shows that the maximum light transmission for a subwavelength aperture height of 160 nm.

After optimizing the subwavelength aperture height, $\mathbf{h_s}$, three parameters of the SPPs-enhanced MSM-PD structure are optimized. These are the nano-grating height, $\mathbf{h_g}$, duty cycle **X%,** and the number of nano-grating pitches. Each parameter was varied over a certain range of values, while all other parameters were kept constant.

a) Nano-grating Height Optimization

By defining a term called light transmission enhancement factor (**Γ**), which is the calculated light transmission of the device with the nano-grating divided by that without the nano-grating, we can give a concise expression for the increase in transmitted flux into the active area for the same device with and without the nano-grating.

Taking the subwavelength aperture height of 160 nm, $\mathbf{x_w}$ of 100 nm, 50% duty cycle, and 4 grating periods, the nano-grating height $\mathbf{h_g}$ was varied from 10 nm to 150 nm in steps of 20 nm. Furthermore, the $\mathbf{h_s}$ was decreased from 150 nm to 10 nm in the same steps to keep the subwavelength aperture height constant at160 nm.

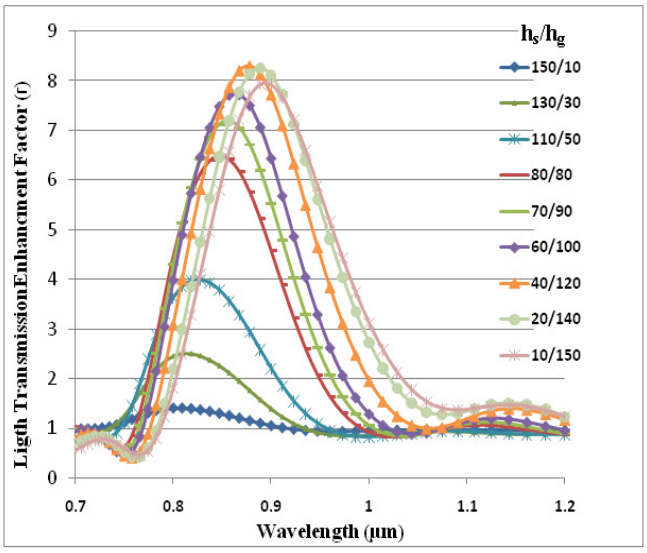

Fig. 2. Light transmission enhancement factor for $\mathbf{x_w}$ = 100 nm for different nano-grating heights.

Fig. 2 shows **Γ** spectrum for different nano-grating heights. The transmission spectra make it apparent that the nano-grating height has a significant impact on the amount of power transmitted into the semiconductor area. The effects of the nano-grating height on the transmitted power into the active area become clearer by plotting the value of the maximum **Γ** as a function of the nano-grating height, as shown in Fig. 3. The maximum **Γ** is obtained at $\mathbf{h_g}$ = 120 nm and $\mathbf{h_s}$ = 40 nm. Another interesting observation can be recognized from these spectra that the central position of the optimum wavelength is red-shifted. The wavelength ($\boldsymbol{\lambda_{max}}$) at which **Γ** is maximum is plotted versus the nano-grating height to elucidate the effects of the nano-grating height as shown in Fig. 4. The maximum **Γ** is at 878 nm, which is not the design wavelength of the nano-grating. However, this wavelength still falls within the absorption range of GaAs, and thus, it is adequate for increasing the transmission through the subwavelength aperture into the active area.

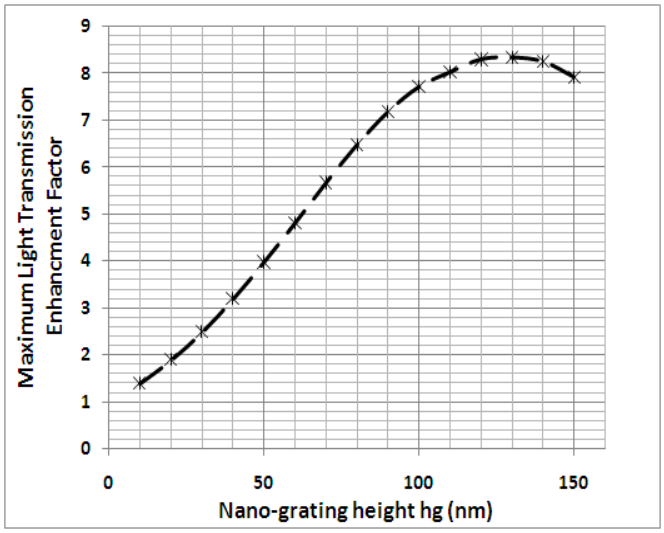

Fig.3. Maximum light transmission enhancement factor versus the nano-grating height, h_g.

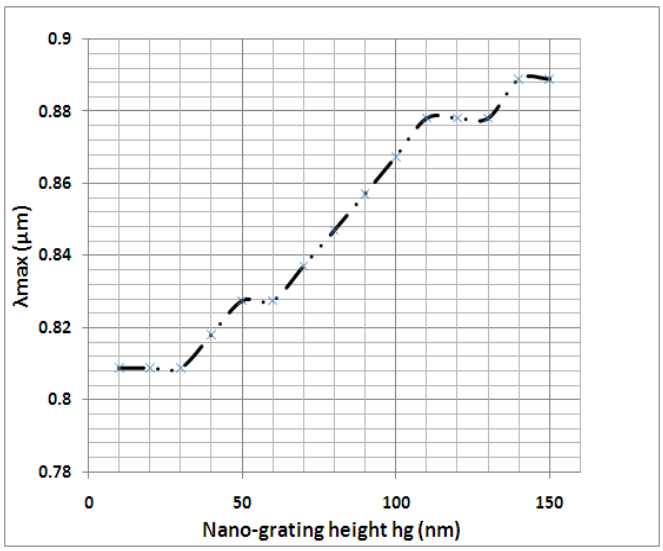

Fig. 4. Peak wavelength (λ_{max}) of maximum light transmission enhancement factor versus the nano-grating height, h_g.

b) Nano-grating Duty Cycle Optimization

The nano-grating duty cycle was varied from 0% to 100% in steps of 10%, while the heights $\mathbf{h_s}$ and $\mathbf{h_g}$ were kept at 40 nm and 120 nm respectively. Fig. 5 shows the **Γ** spectra versus the duty cycle. It is apparent that, as with the nano-grating height, the duty cycle not only affects the amount of the light flux transmitted into the active area, but also the peak wavelength. The maximum **Γ** and the peak wavelength are plotted against the duty cycle in Fig. 6 and Fig. 7, respectively.

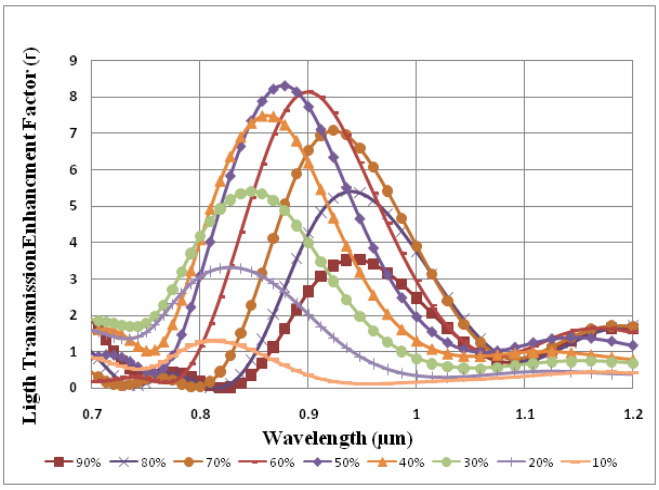

Fig. 5. Light transmission enhancement factor for $\mathbf{x_w}$ = 100 nm with varying nano-grating duty cycle.

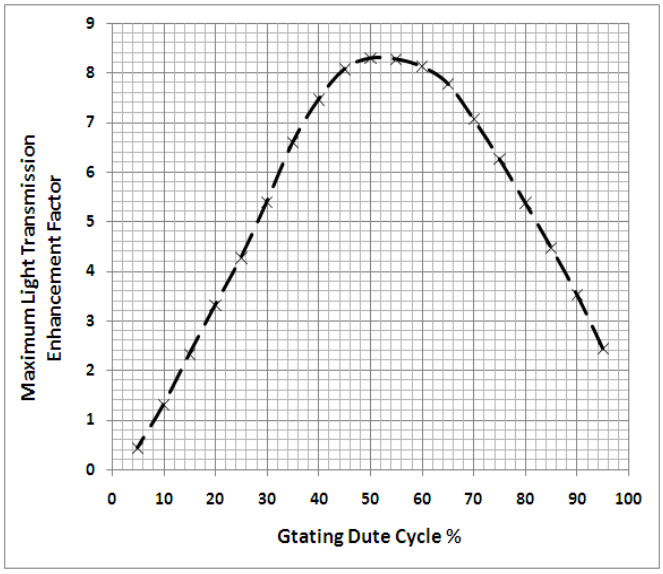

Fig. 6. Maximum light transmission enhancement factor versus the nano-grating duty cycle.

Fig. 6 shows that the maximum **Γ** is relatively steady between 45% and 60%, while the peak wavelength of the maximum enhancement gradually rises between 867 nm and 900 nm (as shown in Fig. 7), which is at the edge of the absorption band of GaAs. For nano-grating duty cycles below 40% and above 65% the maximum **Γ** falls rapidly.

Finally, the impact of the nano-grating period numbers was investigated. The maximum **Γ** was obtained when the number of the nano-grating periods is 7 and 8.

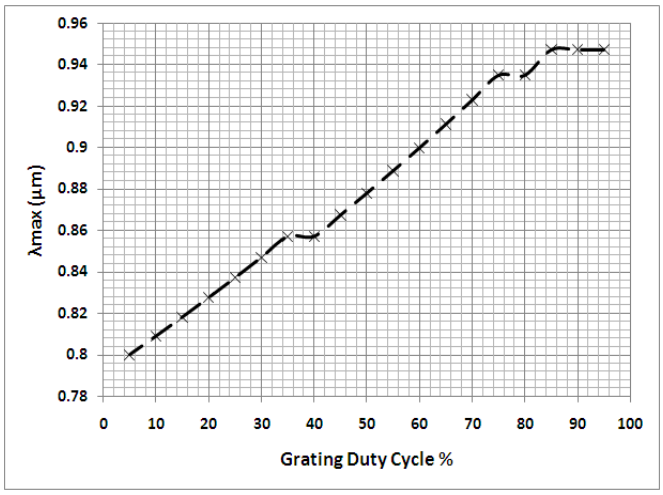

Fig. 7. Peak wavelength (λ_{max}) of maximum light transmission enhancement factor versus the nano-grating duty cycle.

c) Simulation of Optimized Device

The optimized device was subsequently simulated using the parameters determined in the previous sections, which are: i) subwavelength aperture width of 100 nm, ii) nano-grating height of 120 nm, iii) nano-grating duty cycle of 50%, and iv) number of the nano-grating periods of 7. The light enhancement transmission spectrum for the optimized device is shown in Fig. 8.

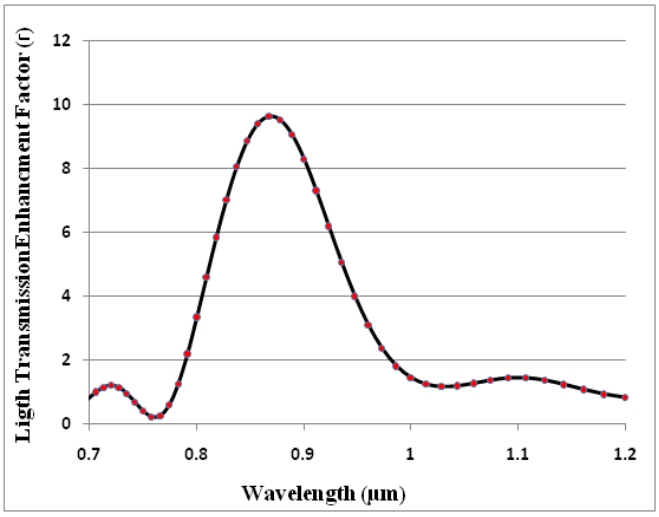

Fig. 8. Light transmission enhancement factor spectrum for the optimized MSM-PD device.

From Fig. 8, it is observed that the light transmission enhancement factor is ~10-times, however, the peak wavelength is shifted to 867 nm. Furthermore, this wavelength is still within the range of absorption spectrum of GaAs.

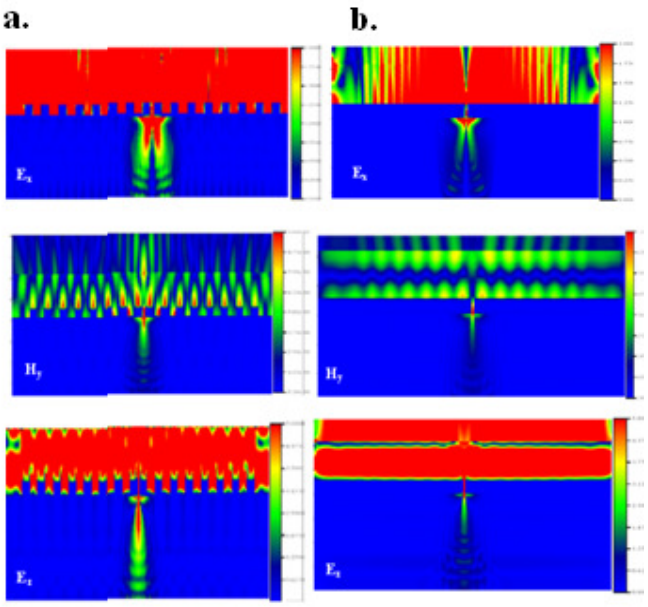

Fig. 9. Field distributions (E_x, H_y and E_z) of the optimized device with (a) and without the nano-grating (b).

The electric and magnetic field distribution components ($\mathbf{E_x}$, $\mathbf{H_y}$, and $\mathbf{E_z}$) for the optimized MSM-PDs with and without the nano-grating are shown Fig. 9. These field distributions clearly show the SPPs coupling effects and the light transmission enhancement through the subwavelength aperture with the incorporation of the nano-grating. Fig. 9 (b) shows that a small fraction of the electric field is transmitted into the active area of the device without the nano-grating. The magnetic field distribution for the MSM-PD with the nano-grating (Fig. 9(a)) shows a significant amount of the total magnetic field is transmitted into the active area. The field distributions for the device with the nano-grating clearly show the presence of a TM polarized wave propagating along the surface, as predicted by the SPPs coupling theory [16]. These simulated field distributions serve as a proof of concept for the SPPs enhanced MSM-PD.

IV. Conclusion

We have designed and simulated the performance of an ultrafast plasmonic MSM-PD device employing a metal nano-grating for the enhancement of light transmission (and hence responsivity-bandwidth product) through a subwavelength aperture. FDTD method has been used to optimize the various device parameters, namely the subwavelength aperture depth, the nano-grating height, the grating duty cycle, and other structure parameters for maximum light transmission enhancement. Simulation results have shown that the plasmonic MSM-PD structure can attain a maximum light transmission enhancement factor of ~10-times better than the achieved with conventional MSM-PD. These simulation results are useful for the development of high-responsivity-bandwidth MSM-PDs.

Acknowledgement

Authors would like to acknowledge the support for this research from the Department of Nano-bio Materials and Electronics, Gwangju Institute of Science and Technology, Republic of Korea.

References

[1] J. B. D. Soole and H. Schumacher, "InGaAs metal-semiconductor-metal photodetectors for long wavelength optical communication," *IEEE J. Quantum Electron.*, vol. 27, no. 3, pp. 737–752, Mar. 1991.

[2] M. Ito and O. Wada, "Low dark current GaAs metal-semiconductormetal (MSM) photodiodes using WSi contacts," *IEEE J. Quantum Electron.*, vol. QE-22, no. 7, pp. 1073–1077, Jul. 1986.

[3] S. Y. Chou, Y. Liu, and P. B. Fischer, "Tera-hertz GaAs metal-semiconductor-metal photodetectors with 25 nm finger spacing and finger width" Appl. Phys. Lett., 61 (4), 27 Jul. 1992.

[4] T. W. Ebbesen, H. J. Lezec, H.F. Ghaemi, T. Thio and P. A. Wolff, "Extraordinary optical transmission throught sub-wavelength hole arrays," Nature, Vol 391, 667–669, 1998.

[5] W. Li-Chun, D. L. Ni, N. Yue-Ping and G. Shang-Qing, "Extraordinary optical transmission throught metal gratings with single and double grooved surfaces," Chin. Phys. B Vol. 19, No. 1 017303, 2010.

[6] R. D. Bhat, N. C. Panoiu, S. R. Brueck, and R. M. Osgood, "Enhancing the signal-to-noise ratio of an infrared photodetector with a circular metal grating," Opt. Exp, Vol. 16, No. 7 , 4588, Mar. 2008.

[7] F. J. García-Vidal and, L. Martín-Moreno, "Transmission and focusing of light in one-dimensional periodically nanostructured metals," Phys. Rev. B, Vol. 66, Issue 155412, 2002.

[8] G. Lévêque, O. J. F. Martin, and J. Weiner, "Transient behavior of surface plasmon polaritons scattered at a subwavelength groove," Phys. Rev. B, Vol. 76, 155418, Oct. 2007.

[9] S. Collin, F. Pardo, R. Teissier, and J. Pelouard, "Efficient light absorption in metal–semiconductor–metal nanostructures," *Appl. Phys. Lett.*, vol. 85(2), Jul. 2004.

[10] C. L. Tan, V. V. Lysak, K. Alameh, and Y. T. Lee, "Absorption enhancement of 980 nm MSM photodetector with a plasmonic grating structure," *Opt. Commun*. 283, pp. 1763-1767, 2010.

[11] J. A. Shackleford, R. Grote, M. Currie, J. E. Spanier, and B. Nabet, "Integrated plasmonic lens photodetector," Appl. Phys. Lett. Vol. 94 (8), 083501, Feb. 2009.

[12] F. J. Garcia-Vidal, "Light passing through subwavelength apertures," Rev. Mod. Phys. Vol. 82, Jan. 2010.

[13] T. Ishi, J. Fujikata, K. Makita, T. Baba, and K. Ohashi, "Si Nano-Photodiode with a Surface Plasmon Antenna," Jpn. J. Appl. Phys., Part 2 44, L364, 2005.

[14] OptiFDTD technical background and tutorial manual, version 8, (2008).

[15] E. D. Palik, "Galllium Arsenide (GaAs)" in Handbook of Optical Constants of Solids, E. D. Palik, ed. (Academic, San Diego, USA, 1985).

[16] G. Gay, O. Alloschery, B.V. Lesegno, J. Weiner, and H. J. Lezec. "Surface Wave Generation and Propagation on Metallic Subwavelength Structures Measured by Far-Field Interferometry," Phys. Rev. Lett, 96(21):213901, Jun. 2006.